Journal of Sound and Vibration (1997) **202**(5), 633–655

A HIERARCHICAL FUNCTIONS SET FOR PREDICTING VERY HIGH ORDER PLATE BENDING MODES WITH ANY BOUNDARY CONDITIONS

O. Beslin and J. Nicolas

Groupe d'Acoustique de l'Université de Sherbrooke, Département de Génie Mécanique, Université de Sherbrooke, Sherbrooke, QC, J1K 2R1, Canada

(*Received* 20 *May* 1996, *and in final form* 14 *October* 1996)

In this paper a new hierarchical functions set is proposed to predict flexural motion of plate-like structures in the medium frequency range. This functions set is built from trigonometric functions instead of polynomials as classically encountered in the literature. It is shown that such a trigonometric set presents all the advantages of a classical hierarchical polynomials set and additional ones which are of interest if very high order functions are intended to be used. It is stated that this new trigonometric set can be used at very high orders, up to 2048 without taking care of computer round-off errors, while the polynomials set fail, at order 46 because of the limited numerical dynamics of computers. This trigonometric set can be easily implemented on a computer. It does not require quadruple precision pre-computed arrays. Only a very low number (which does not depend on the function order) of basic operations is needed when calling such functions. Moreover, it is shown that this trigonometric set presents a better convergence rate than polynomials when predicting high order natural flexural modes of rectangular plates with any boundary conditions.

1. INTRODUCTION

The p-version of the finite element method has been of growing interest over the past 25 years. In the p-version of the finite element method, the mesh of the structure is fixed and the degree p of the interpolation functions is progressively increased until the desired degree of convergence is reached. The p-version of the finite element method presents many advantages compared with the classical finite element method (called the h-version, in which h is the maximum diameter of the element). (1) The mesh of the structure has to be generated one time for all; then convergence is reached by increasing the p-order. (2) Input data can be reduced to the minimum, which greatly simplifies pre-post-processing. (3) Adaptative processes for reaching convergence can be realized by increasing automatically the order p, which is easier than adaptative meshing.

A particular class of the p-version of the finite element method, the so-called Hierarchic Finite Elements Method (HFEM), presents a supplementary advantage, which is that the interpolation functions set of order p_{max} constitutes a subset of the interpolation functions set of order $(p_{max} + 1)$. Consequently, the mass and stiffness matrix elements which were calculated for the (p) order set can be re-used for the $(p + 1)$ order set. This is the reason why such elements are called "*hierarchical*". Many authors have explored the p-version of the finite element method [1–6]. They have demonstrated its superior efficiency to reach

0022–460X/97/200633 + 23 $25.00/0/sv960797

convergence [3, 7], and to deal with singularities [3] in comparison with the classical h-version of the finite element method.

HFEM seems to be an attractive method to treat vibrations problems in the mid-frequency range where the structure's vibratory fields have very short wavelengths but where they are not yet sufficiently diffused to be described with statistical analysis methods [8]. Reaching mid-frequency range with classical FEM seems to be quite difficult as, using six nodes per wavelength, it leads to huge unmanageable data sets. Moreover, in the mid-frequency range, it is not always useful to obtain all displacements over a very fine grid, as in practice they are not measured with so much detail. Only mean quadratic displacement over small surfaces (having the length of some wavelengths) are needed. Using HFEM, such mean information could be obtained by using an ordinary mesh and very high order interpolation functions sets. Then output data could contain only mean quadratic levels over the ordinary mesh elementary surfaces.

Unfortunately boosting HFEM to very high order seems to be difficult. In practice, interpolation functions are polynomials constructed from Jacobi polynomials [9], integrated Legendre polynomials [2, 3, 10–12] or the natural Taylor's basis $\{x^n\}$ [13]. As has been pointed out in the literature, the calculation of high order polynomials coefficients require great care due to computer's round-off errors. That is why some authors have used symbolic computing to calculate high order polynomials coefficients and matrix elements [9–12]. To the author's knowledge, the highest p degree which has been treated using HFEM is 19 [12]. Actually, symbolic computing permits one to circumvent round-off errors when calculating polynomial coefficients, and matrix elements; however, as will be shown in this paper, even if one takes care of the computation of elements, very high order polynomials ($p > 45$) will lead to ill-conditioned mass and stiffness matrices because of the high numerical dynamics of the polynomial coefficients and the limited numerical dynamics of the computers used.

In this paper a new hierarchical interpolation functions set is proposed which permits one to reach the mid-frequency range without being restrained by the limited numerical dynamics of the computer and which requires no particular care of round-off errors. The key to the numerical stability of this new functions set is very simple. The maximum approximation order p_{max} of a functions set is not related to the power of a polynomial but to the number of oscillations of a trigonometric function. Thus, the p_{max} order seems to have no limitations when implementing this trigonometric set on a computer. This trigonometric set also presents other advantages. (1) The inner smoothness of the solution is ensured, as these functions are indefinitely derivable. (2) Mass and stiffness matrix elements are given by exact analytical expressions which are easy to calculate, so that no pre-computed arrays are needed. (3) No recursive formula are used, so that cumulative errors do not occur. (4) For bending problems, this trigonometric set presents "*natural wavelengths*" which permit a better convergence rate for high order structure modes.

This paper is organized as follows: in section 2, a classical hierarchic polynomials set built from integrated Legendre polynomials introduced by Zhu [2] and recently used by Bardell [10–12] is presented. Bardell's work [10] on the rectangular flat plate with any boundary conditions is summarized. Then, it is shown that this polynomials set leads to numerical problems when very high order ($p > 45$) polynomials are considered. In section 3, the proposed trigonometric set is presented and compared with the polynomials set. It is found that this trigonometric set is numerically more stable than the polynomials set. In section 4, the convergence rates of the polynomials set and the trigonometric set are compared in the particular cases of simply supported and free rectangular plates. It is shown that in both cases, the trigonometric set permits a better convergence rate for high

order modes. A very simple wavelength criterion is pointed out which allows one to use this trigonometric set with good accuracy.

2. POLYNOMIALS SET

In this section, a hierarchic polynomials set is presented. This polynomials set is built from integrated Legendre polynomials. To the knowledge of the authors, this polynomials set was initially presented by Zhu [2]. More recently, Bardell has used this set to predict natural flexural vibrations of rectangular plates [10] and skew plates [12]. The plate is considered as a single hierarchical finite element, and boundary conditions such as "simply supported", "clamped", "free" and even "point supported/clamped in corners" can be taken into account by a judicious selection of the basis functions.

2.1. PRESENTATION OF THE HIERARCHIC POLYNOMIALS SET

The Legendre orthogonal polynomials can be expressed using Rodrigues' formula [14] as

$$P_m(\xi)=\frac{1}{m!(-2)^m}\frac{\mathrm{d}^m}{\mathrm{d}\xi^m}\{(1-\xi^2)^m\},\qquad \xi\in[-1,1]. \tag{1}$$

Legendre polynomials satisfy the orthogonal relation

$$\int_{-1}^{1} P_m(\xi)P_n(\xi)\,\mathrm{d}\xi=\frac{2}{2n+1}\,\delta_{nm}. \tag{2}$$

By expanding equation (1) using the binomial theorem, the following explicit expression can be obtained [2]:

$$P_m(\xi)=\sum_{n=0}^{m/2}\frac{(-1)^n}{2^n n!}\frac{(2m-2n-1)!!}{(m-2n)!}\,\xi^{m-2n}, \tag{3}$$

where $m!!=m(m-2)\ldots(2 \text{ or } 1)$, $0!!=1$, $(-1)!!=1$, and $m/2$ denotes its own integer part.

Let $P_m^s(\xi)$ denotes the following s-multiple integral of $P_{m-s}(\xi)$:

$$P_m^s(\xi)=\int_{-1}^{\xi}\cdots\int_{-1}^{\xi}P_{m-s}(\xi)\,\underbrace{\mathrm{d}\xi\ldots\mathrm{d}\xi}_{s-\text{time}}. \tag{4}$$

Substituting equation (3) into equation (4), the following explicit expression for $P_m^s(\xi)$ is obtained:

$$P_m^s(\xi)=\sum_{n=0}^{m/2}\frac{(-1)^n}{2^n n!}\frac{(2m-2n-2s-1)!!}{(m-2n)!}\,\xi^{m-2n}. \tag{5}$$

To the author's knowledge, this last $P_m^s(\xi)$ polynomials set has been first presented by Zhu [2].

$\{P_m^s(\xi)\}$ polynomials sets are of interest since they can be used as hierarchical shape functions of C^{s-1} continuity as all their derivatives of order lower than s vanish at $\xi=\pm 1$.

TABLE 1

The first ten Bardell's polynomials (using doubly integrated Legendre polynomials for order greater than 4)

$f_1(\xi)=\frac{1}{2}-\frac{3}{4}\xi+\frac{1}{4}\xi^3$	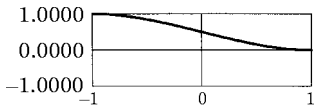
$f_2(\xi)=\frac{1}{8}-\frac{1}{8}\xi-\frac{1}{8}\xi^2+\frac{1}{8}\xi^3$	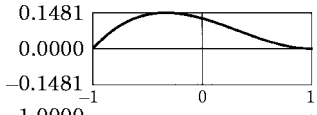
$f_3(\xi)=\frac{1}{2}+\frac{3}{4}\xi-\frac{1}{4}\xi^3$	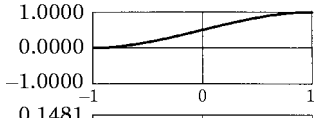
$f_4(\xi)=-\frac{1}{8}-\frac{1}{8}\xi+\frac{1}{8}\xi^2+\frac{1}{8}\xi^3$	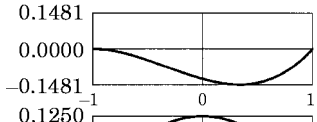
$f_5(\xi)=\frac{1}{8}-\frac{1}{4}\xi^2+\frac{1}{8}\xi^4$	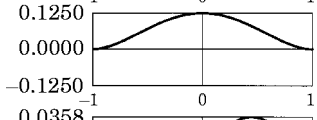
$f_6(\xi)=\frac{1}{8}\xi-\frac{1}{4}\xi^3+\frac{1}{8}\xi^5$	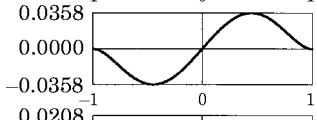
$f_7(\xi)=-\frac{1}{48}+\frac{3}{16}\xi^2-\frac{5}{16}\xi^4+\frac{7}{48}\xi^6$	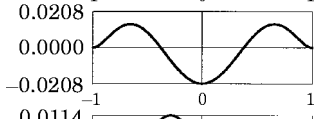
$f_8(\xi)=-\frac{3}{48}\xi+\frac{5}{16}\xi^3-\frac{7}{16}\xi^5+\frac{9}{48}\xi^7$	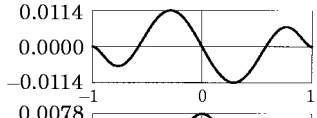
$f_9(\xi)=\frac{3}{384}-\frac{15}{96}\xi^2+\frac{35}{64}\xi^4-\frac{63}{96}\xi^6+\frac{99}{384}\xi^8$	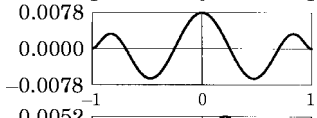
$f_{10}(\xi)=\frac{15}{384}\xi-\frac{35}{96}\xi^3+\frac{63}{64}\xi^5-\frac{99}{96}\xi^7+\frac{143}{384}\xi^9$	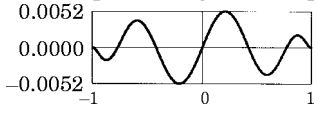

2.2. APPLICATION TO PURE BENDING MODE SHAPES OF A RECTANGULAR PLATE

Bardell [10] has proposed a hierarchical polynomials set dedicated to plate bending problems. He built a hierarchical shape functions of C^1 continuity from Zhu's polynomials $\{P_m^s(\xi)\}$, considering the particular value $s = 2$ [2].

2.2.1. *Bardell's polynomials set*

Bardell [10] has predicted bending modes of a rectangular plate (with any boundary conditions) by considering the rectangular plate as a single element and a hierarchical polynomials set. A first part of this polynomials set is built from the classical FEM first four cubic displacement functions:

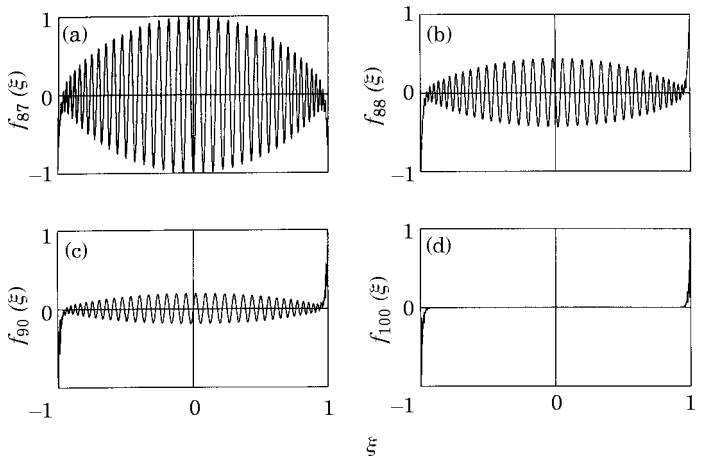

Figure 1. Round-off errors when calculating high order Bardell's polynomials. (a) Order 87; (b) order 88; (c) order 90; (d) order 100.

$$f_1(\xi) = \tfrac{1}{2} - \tfrac{3}{4}\xi + \tfrac{1}{4}\xi^3, \qquad f_2(\xi) = \tfrac{1}{8} - \tfrac{1}{8}\xi - \tfrac{1}{8}\xi^2 + \tfrac{1}{8}\xi^3, \tag{6, 7}$$

$$f_3(\xi) = \tfrac{1}{2} + \tfrac{3}{4}\xi - \tfrac{1}{4}\xi^3, \qquad f_4(\xi) = -\tfrac{1}{8} - \tfrac{1}{8}\xi + \tfrac{1}{8}\xi^2 + \tfrac{1}{8}\xi^3. \tag{8, 9}$$

A second part of the polynomials set is built from equation (5), with $s = 2$, as follows:

$$f_r(\xi) \equiv P^{s=2}_{m=r-1}(\xi) = \sum_{n=0}^{(r-1)/2} \frac{(-1)^n}{2^n n!} \frac{(2r-2n-7)!!}{(r-2n-1)!} \xi^{r-2n-1}, \qquad r > 4. \tag{10}$$

This basis set used by Bardell is summarized in Table 1. It can be seen that all functions of the higher part of the basis set ($r > 4$) have zero displacement and zero slope at each end of the element (because of the use of $s = 2$ in equation (5)). Consequently, boundary conditions on displacement and rotation at the edges of the plate are entirely controlled by the first four basis functions. Thus, particular boundary conditions such as simply supported, clamped and point supported/clamped in corners can be treated only by removing some basis functions from this polynomials set.

2.2.2. *Natural modes of a rectangular plate with any boundary conditions*

Consider a flat homogeneous rectangular plate in pure bending motion. In Cartesian co-ordinates, the plate domain is $\mathscr{S} = \{M(x, y)/(x, y) \in [0, a] \times [0, b]\}$. The plate normal displacement is sought as an expansion on Bardell's basis $\{f_r(\xi)\}$ (given in Table 1):

$$w(\xi, \eta) = \sum_{r=1}^{p} \sum_{s=1}^{p} q_{rs} f_r(\xi) f_s(\eta), \tag{11}$$

where ξ and η are non-dimensional parameters such that $x = (1 + \xi)a/2$ and $y = (1 + \eta)b/2$. The strain and kinetic energy are classically expressed for pure bending thin plates and small displacements as

$$U = \tfrac{1}{2} \frac{4Db}{a^3} \int_{-1}^{1} \int_{-1}^{1} \left[\left(\frac{\partial^2 w}{\partial \xi^2} \right)^2 + \left(\frac{a}{b} \right)^4 \left(\frac{\partial^2 w}{\partial \eta^2} \right)^2 + 2\nu \left(\frac{a}{b} \right)^2 \left(\frac{\partial^2 w}{\partial \xi^2} \right) \left(\frac{\partial^2 w}{\partial \eta^2} \right) \right.$$

$$+ 2(1-\nu)\left(\frac{a}{b}\right)^2\left(\frac{\partial^2 w}{\partial\xi\partial\eta}\right)^2\Bigg]\mathrm{d}\xi\,\mathrm{d}\eta, \tag{12}$$

$$T = \tfrac{1}{2}\frac{\rho hab}{4}\int_{-1}^{1}\int_{-1}^{1}\left(\frac{\partial w}{\partial t}\right)^2\mathrm{d}\xi\,\mathrm{d}\eta, \tag{13}$$

where h is the plate thickness, ρ is the plate density, ν is the plate Poisson ratio, E is Young's modulus and D is the classical flexural rigidity.

The unknown coefficients q_{rs} relative to the free motion of the plate are determined from Lagrange's equations:

$$\frac{\partial U}{\partial q_{rs}} + \frac{\mathrm{d}}{\mathrm{d}t}\frac{\partial T}{\partial \dot{q}_{rs}} = 0, \qquad \text{for } r = 1, 2, \ldots, p,\ s = 1, 2, \ldots, p. \tag{14}$$

Substituting equations (11), (12) and (13) into equation (14), the classical eigenvalues problem is obtained:

$$[k_{jkrs}]\{q_{rs}\} = \omega^2[M_{jkrs}]\{q_{rs}\}, \tag{15}$$

where $[M]$ and $[K]$ are the mass and stiffness matrices, and where

$$M_{jkrs} = \frac{\rho hab}{4} I_{jr}^{00} I_{ks}^{00}, \tag{16}$$

$$K_{jkrs} = \frac{4Db}{a^3}\left[I_{jr}^{20} I_{ks}^{20} + \left(\frac{a}{b}\right)^4 I_{jr}^{02} I_{ks}^{02} + \nu\left(\frac{a}{b}\right)^2 (I_{jr}^{20} I_{ks}^{02} + I_{jr}^{02} I_{ks}^{20}) + 2(1-\nu)\left(\frac{a}{b}\right)^2 I_{jr}^{11} I_{ks}^{11}\right], \tag{17}$$

in which integrals $I_{jr}^{\alpha\beta}$ are defined by

$$I_{jr}^{\alpha\beta} = \int_{-1}^{1} f_j^{(\alpha)} f_r^{(\beta)}\,\mathrm{d}\xi, \tag{18}$$

where (α) and (β) denote the order of derivatives ($\alpha, \beta = 0, 1, 2$).

Bardell has used this formulation to predict free vibrations of rectangular plates with ten different boundary conditions (including point support). He has validated his approach in comparison with literature results [15–19] for the first four flexural modes, using the first ten basis functions presented in Table 1. He has used symbolic computing [11] to calculate polynomials coefficients and integrals $I_{jr}^{\alpha\beta}$ defined in equation (18).

It was interesting to boost this method to higher orders to predict more than the first four flexural modes. Thus, the authors have implemented this method in a FORTRAN program to test it at higher orders.

2.3. NUMERICAL LIMITATIONS OF THE POLYNOMIALS SET

2.3.1. *Implementing Bardell's approach in a FORTRAN program*

The polynomial coefficients given in equation (10) were calculated in quadruple precision while taking care systematically to simplify integers quotients, term by term, each time that it was possible (as is done in symbolic computing software). Mass and stiffness elements were also assembled in quadruple precision. Then, the eigenvalues problem (15) was solved in double precision using EISPACK package FORTRAN routines. It was found that the polynomials set $\{f_r(\xi)\}$ could be boosted up to order $p = 45$. For orders higher than 45,

mass and stiffness matrices were found to be ill-conditioned. The origin of this numerical problem can be explained more deeply as shown in the following sections.

2.3.2. *Large numerical dynamic of the coefficients*

In Figure 1 very high order $f_r(\xi)$ polynomials are plotted, for four different values of r ((a) $r = 87$, (b) $r = 88$, (c) $r = 90$ and (d) $r = 100$). In Figure 1(a), it can be seen that $f_{87}(\xi)$ presents some errors at both ends, $\xi = \pm 1$. In Figures 1(b)–(d) it is shown that these errors are growing with the order r and that their magnitudes become greater than the maximum magnitude of the exact function. It is to be noted that integral terms $I_{jr}^{\alpha\beta}$ defined in equation (18) are precisely calculated from integrated polynomial values at both ends $\xi = \pm 1$, and consequently they also become erroneous for very high order r.

Erroneous values at both ends are due to the very large numerical dynamic of polynomial coefficients. Actually, as can be seen in equation (10), $f_r(\xi)$ polynomial coefficients are defined by the factorial functions ratio. This leads to a very high dynamic between the smaller and the greater coefficient of a high order polynomial. This effect is described in Figure 2, where the coefficients of four different $f_r(\xi)$ polynomials are plotted. It can be seen that for $r = 10$ (as in Bardell's work [10]), the coefficients numerical dynamic is less than 100, so that numerical problems do not occur. However, for $r = 45$, the coefficients numerical dynamic is near 10^{16}. Using double precision, a computer round-off error is precisely situated between 10^{-17} and 10^{-16} (it is machine dependent). Therefore, it is clear that in such a case, even if polynomial coefficients and mass/stiffness matrix elements are calculated exactly and rigorously, any eigenvalues problem (or linear system resolution) software will fail to find eigenvectors (or solution vectors).

2.3.3. *Numerically non-positive definite scalar product*

Another way to show that $f_r(\xi)$ polynomials cannot be used at very high orders is that, theoretically, the matrix I_{jr}^{00} (defined in equation (18)) represents a scalar product, so theoretically I_{jr}^{00} is symmetric positive definite and must have only real positive non-zero

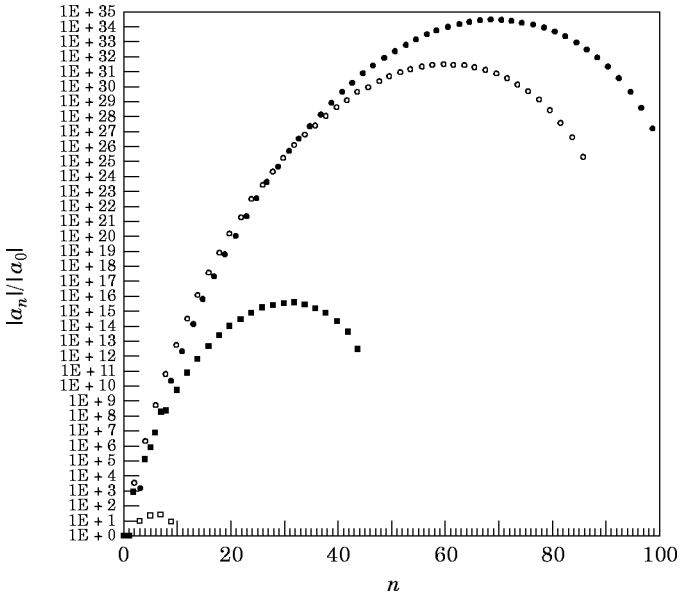

Figure 2. The numerical dynamic of coefficients a_n relative to Bardell's polynomials. a_n are such that $f_r(\xi) = \Sigma_{n=0}^{r-1} a_n \xi^n$: □, $r = 10$; ■, $r = 45$; ○, $r = 87$; ●, $r = 100$.

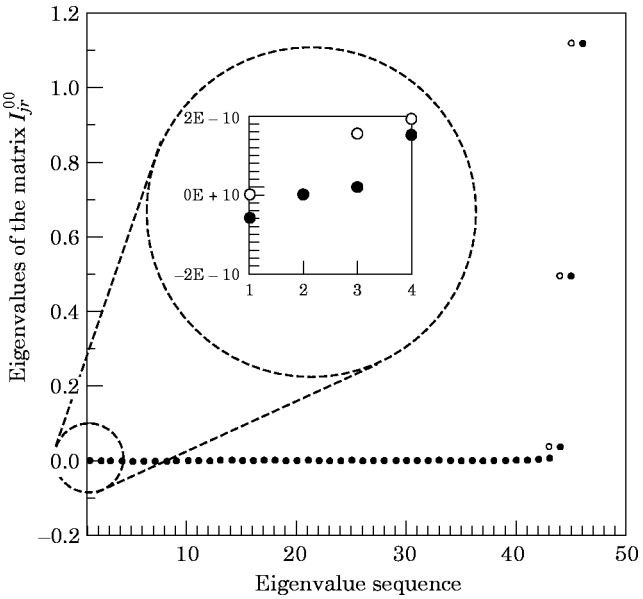

Figure 3. Eigenvalues of the matrix I_{jr}^{00}. ○, Using the first 45 Bardell's polynomials; ●, using the first 46 Bardell's polynomials.

eigenvalues. However, numerically as summarized in Figure 3, solving the eigenvalues problem of I_{jr}^{00}, negative eigenvalues can be found. In Figure 3 two different sets of eigenvalues are reported, relative to two different $\{f_r(\xi)\}$ polynomials bases; a first $\{f_r(\xi)\}$ set containing $f_r(\xi)$ functions for $r = 1$ to 45, and a second set containing $f_r(\xi)$ functions for $r = 1$ to 46. It can be seen that in the case $r = 1$ to 46, the first eigenvalue is a negative one, so I_{jr}^{00} is no longer numerically positive definitive. This is the reason why the free vibrations problem relative to the rectangular plate defined in equation (15) was failing for $r > 45$.

TABLE 2

Table of coefficients (a_r, b_r, c_r, d_r) *relative to the trigonometric set* $\{\psi_r(\xi)\}$ (*where* $\psi_r(\xi) = \sin(a_r\xi + b_r)\sin(c_r\xi + d_r)$)

Order r	Coefficient, a_r	Coefficient, b_r	Coefficient, c_r	Coefficient, d_r
1	$\frac{\pi}{4}$	$\frac{3\pi}{4}$	$\frac{\pi}{4}$	$\frac{3\pi}{4}$
2	$\frac{\pi}{4}$	$\frac{3\pi}{4}$	$-\frac{\pi}{2}$	$-\frac{3\pi}{2}$
3	$\frac{\pi}{4}$	$-\frac{3\pi}{4}$	$\frac{\pi}{4}$	$-\frac{3\pi}{4}$
4	$\frac{\pi}{4}$	$-\frac{3\pi}{4}$	$\frac{\pi}{2}$	$-\frac{3\pi}{2}$
r > 4	$\frac{\pi}{2}(r-4)$	$\frac{\pi}{2}(r-4)$	$\frac{\pi}{2}$	$\frac{\pi}{2}$

In summary, Bardell's polynomials set $\{f_r(\xi)\}$ is of interest since all functions of order higher than four have no influence on the boundary conditions relative to displacement and rotation. Moreover, this set is a hierarchical one. However, it is stated that the use of such polynomials is limited to a maximum order of 45 since they present too large a numerical dynamic of their coefficients.

3. A TRIGONOMETRIC SET

The authors were interested in having a hierarchical functions set similar to the one proposed by Bardell, but that could be used to higher order than 45 and without being constrained to take care of numerical round-off errors. It was found that such a basis can be built from trigonometric functions.

3.1. BUILDING A HIERARCHICAL SET WITH TRIGONOMETRIC FUNCTIONS

Consider the trigonometric set $\{\psi_r(\xi)\}$ defined as

$$\psi_r(\xi) = \sin(a_r\xi + b_r)\sin(c_r\xi + d_r), \qquad r = 1, 2, \ldots, \tag{19}$$

where the coefficients a_r, b_r, c_r and d_r are given in Table 2.

The first ten functions $\psi_r(\xi)$ defined by equation (19) are reported in Table 3, in comparison with the ten first Bardell polynomials $f_r(\xi)$. In terms of shapes, this proposed trigonometric set presents the same tendency as Bardell's polynomials: (1) the first four functions permit one to satisfy any boundary conditions; (2) all functions of order higher than four have zero displacement and zero slope at both ends $\xi = \pm 1$; (3) for $r > 4$, these functions have a number "$r - 5$" of simple roots in the inner domain $]-1, +1[$.

3.2. COMPARISON BETWEEN THE TRIGONOMETRIC SET AND THE POLYNOMIALS SET

This trigonometric set presents the advantages of Bardell's polynomials and interesting additional ones. As the order of a $\psi_r(\xi)$ function is not related to a power of ξ but to the number of oscillations of a trigonometric function it is numerically more stable than polynomials.

First, round-off errors at both ends $\xi = \pm 1$ do not occur. In Figure 4, the functions $\psi_{100}(\xi)$ and $\psi_{2048}(\xi)$ are plotted. It can be observed that these functions actually have zero displacement and slope at both ends, $\zeta = \pm 1$. It is to be noted that the function $\psi_{2048}(\xi)$ has been plotted only in the domain $[-1, -0{\cdot}98]$ in order to see details that cannot be observed when plotting it in the full domain $[-1, 1]$.

Second, the $\{\psi_r(\xi)\}$ set leads to well conditioned matrices, even considering very high order functions. Using very high order trigonometric functions $\{\psi_r(\xi)\}$ instead of polynomials $\{f_r(\xi)\}$ in the definition (18) of the matrix I_{jr}^{00}, a numerically symmetric positive definitive matrix is actually obtained. In Figure 5, the eigenvalues of the matrix I_{jr}^{00} using 2048 trigonometric functions are plotted. It can be seen that all the eigenvalues are real and strictly positive. Therefore, in opposition with polynomials, it is stated that this new I_{jr}^{00} matrix actually represents a scalar product up to order 2048 (at least), when polynomials fail for $r = 46$. It is noted that this 2048×2048 I_{jr}^{00} matrix was assembled using only double precision and not quadruple precision as for the polynomials set. Therefore, definitely, the trigonometric set is numerically more stable than the polynomials set.

A third addtitional advantage of the $\{\psi_r(\xi)\}$ trigonometric set is that a very low number of basic operation are required to calculate it. Looking at the definition (19) of ψ_r, it can be seen that only two additions, two multiplications and two calls to intrinsic functions

TABLE 3

A comparison between the trigonometric set and the polynomials set

Function	Trigonometric set $\psi_r(\xi)$	Polynomials set $f_r(\xi)$
1	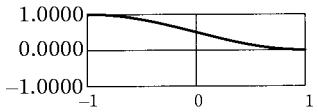	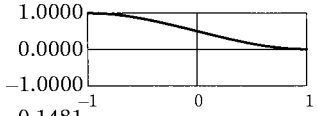
2	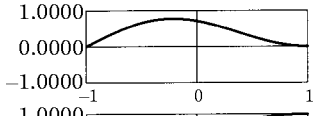	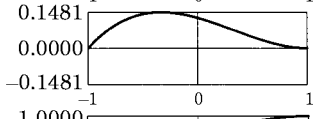
3	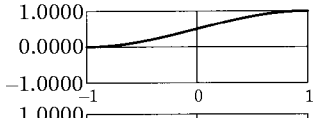	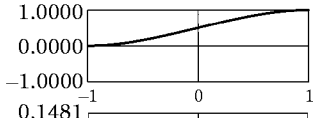
4	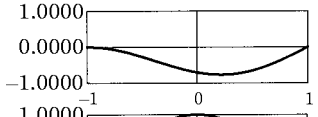	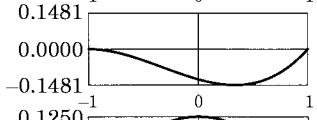
5	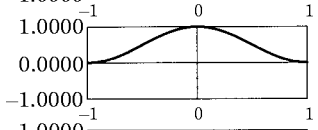	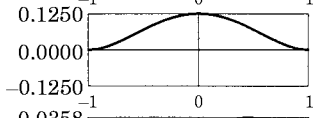
6	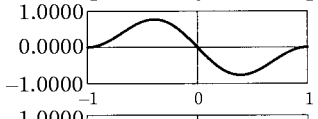	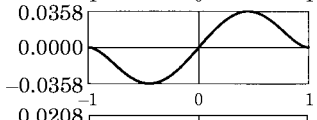
7	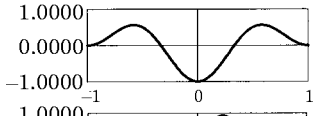	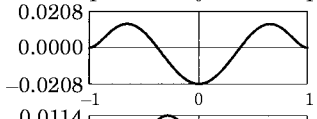
8	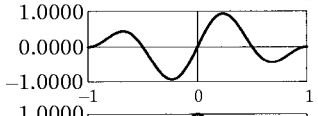	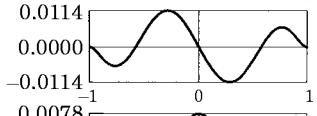
9	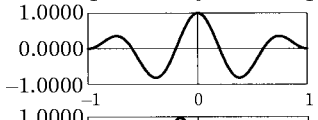	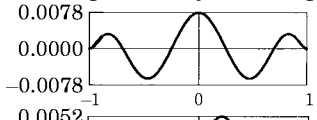
10	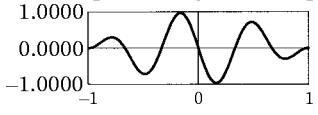	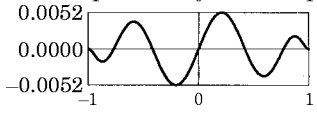

are needed for any values of the order r. At the opposite extreme, using a polynomials set, the number of basic operations is increasing with the order r and a large number of coefficients have to be stored into pre-computed arrays. Therefore, using trigonometric functions, running time and memory are saved.

It has been shown in this section that the proposed trigonometric set $\{\psi_r(\xi)\}$ is very close to Bardell's polynomials $\{f_r(\xi)\}$ in terms of shapes, but it is numerically greatly more stable than the polynomials. Moreover, a high order $\{\psi_r(\xi)\}$ trigonometric set can be implemented in a program in an easier way than polynomials.

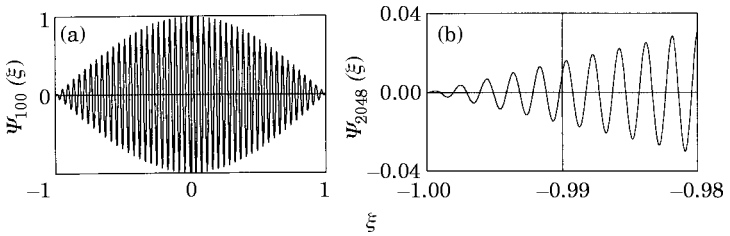

Figure 4. An example of high order trigonometric functions $\psi_r(\xi)$ for (a) $r = 100$, and (b) $r = 2048$.

4. APPLICATION TO THE RECTANGULAR PLATE FLEXURAL VIBRATIONS

Being numerically stable is not the only condition that is required. It must be verified that the trigonometric set is sufficiently complete to allow the convergence of all the natural modes of the structure. It will be shown in this section that the $\{\psi_r(\xi)\}$ set permits actually to predict natural modes, in particular cases of a simply supported plate and a free plate. Also, convergence rates of the $\{\psi_r(\xi)\}$ and $\{f_r(\xi)\}$ sets will be compared. It must be mentioned that, strictly, the equations that govern the plate motion at low frequencies are not valid in the mid-frequency range. Other effects, such as rotational inertia and shear deformation, will now be present which will modify the vibrational behaviour quite significantly. These effects are neglected in this paper, as the principal aim is to provide a simple comparison with other work. However, if a serious analysis of a flat plate at such frequencies is to be undertaken, then the additional effects mentioned will have to be included.

4.1. GENERAL CONSIDERATIONS

4.1.1. *The studied plate*

In both following sections, a rectangular steel plate will be considered with two different configurations of boundary conditions. A first configuration has all edges simply supported (denoted S–S–S–S), and a second one has all edges free (denoted F–F–F–F). The geometrical and mechanical characteristics of the studied plate are: the plate dimensions

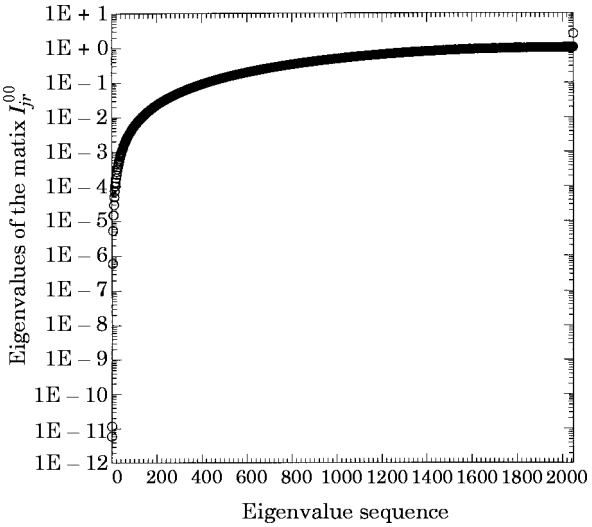

Figure 5. Eigenvalues of the matrix I_{jr}^{00} using the first 2048 trigonometric functions $\{\psi_r(\xi)\}$.

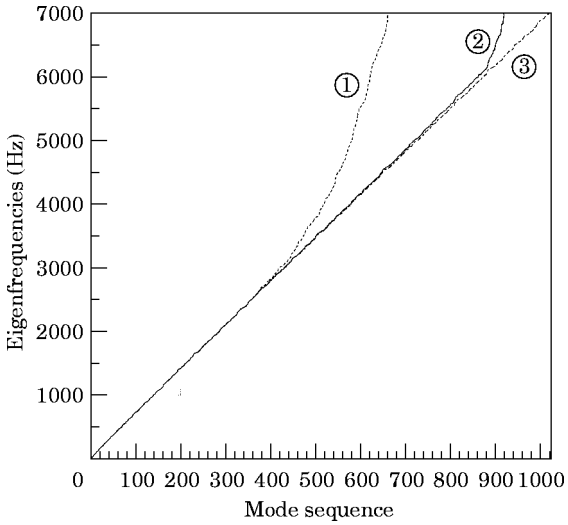

Figure 6. The convergence of eigenfrequencies of a S–S–S–S plate using polynomials (①) and trigonometric (②) sets of 1024 basis functions. (③ is analytical reference).

are, $a = 1{\cdot}4$ m, $b = 1$ m, $h = 0{\cdot}003$ m; Young's modulus, $E = 2 \times 10^{11}$ Pa; Poisson ratio, $v = 0{\cdot}3$; and density, $\rho = 7800\ \mathrm{kg\,m^{-3}}$.

4.1.2. *Selection of the two-dimensional basis functions*

Let us denote by r and s the indices relative to the x-axis and y-axis when expanding the plate normal displacement on the $\{\psi_r(\xi)\}$ or $\{f_r(\xi)\}$ set. In both cases, the normal displacements can be expressed as

$$w(\xi, \eta) = \sum_{(r,s)\in\Omega} q^f_{rs} \tilde{f}_{rs}(\xi, \eta) \tag{20}$$

or

$$w(\xi, \eta) = \sum_{(r,s)\in\Omega} q^\psi_{rs} \tilde{\psi}_{rs}(\xi, \eta), \tag{21}$$

where $\{\tilde{f}_{rs}(\xi, \eta)\}$ or $\{\tilde{\psi}_{rs}(\xi, \eta)\}$ are two-dimensional functions built from the $\{f_r(\xi)\}$ or $\{\psi_r(\xi)\}$ set, respectively, as follows:

$$\tilde{f}_{rs}(\xi, \eta) \equiv f_r(\xi) f_s(\eta), \qquad \tilde{\psi}_{rs}(\xi, \eta) \equiv \psi_r(\xi)\psi_s(\eta), \tag{22, 23}$$

and where Ω denotes the set of selected values of couples (r, s).

In the selection of (r, s) couples, the authors have not chosen the "*square selection*" proposed by Bardell, $\Omega \equiv \{(r, s) \in [1, 2, \ldots, 10] \times [1, 2, \ldots, 10]\}$. For a better convergence, they have used a "*quarter disc selection*" which can be summarized as follows.

Let one denote by N_r the number of simple roots of the $\psi_r(\xi)$ or $f_r(\xi)$ function in the inner domain $]-1, 1[$ (for example, in Table 3, the $\psi_8(\xi)$ and $f_8(\xi)$ functions have three simple roots in the inner domain $]-1, 1[$). The set Ω of the retained couple (r, s) is

$$\Omega \equiv \left\{(r, s) \text{ such that } \left(\frac{N_r + 1}{a}\right)^2 + \left(\frac{N_s + 1}{b}\right)^2 \leqslant k^2_{max}\right\}, \tag{24}$$

where k_{max} is a constant that can be adjusted, depending on the number of basis functions $\psi_r(\xi)$ or $f_r(\xi)$ that are to be used.

4.2. THE S–S–S–S PLATE

Looking at Table 3, it is evident that the case of the simply supported plate can be treated by only removing functions of order $r = 1$ and $r = 3$ from the full set. Then the natural modes of the S–S–S–S plate can be calculated by solving the eigenvalues problem (15). It was done with a trigonometric set $\{\tilde{\psi}_{rs}(\xi, \eta)\}$ and a Bardell's polynomial set $\{\tilde{f}_{rs}(\xi, \eta)\}$, both containing 1024 basis functions, selected using criterion (24) (excluding $r, s = 1$ and $r, s = 3$). The convergence of both approaches is discussed in the followng sections.

4.2.1. *Convergence of eigenfrequencies*

In Figure 6, the eigenfrequencies obtained using the polynomials and the trigonometric set are reported and compared with the classical analytical solution. It can be seen that the trigonometric set allows a better convergence than the polynomials set. Convergence of eigenfrequencies is satisfying up to 6000 Hz (880th mode) with the trigonometric set, while the polynomials set only reaches modes up to the 400th mode (2800 Hz). This difference in convergence rate can be explained in terms of the "*minimum wavelength*" contained in the functions set, as shown in the next section.

4.2.2. *Minimum wavelength criterion*

By choosing 1024 basis functions following criterion (24), the maximum order r is found to be 44. In Figure 7, the trigonometric functions ψ_{44} and the polynomial f_{44} are plotted. It can be seen that these two functions are very similar; however, there is one important difference. As the trigonometric function is built from sine functions, there is a constant step between two successive roots. The polynomials set is built from integrated Legendre polynomials and it can be observed that there is not a constant distance between two

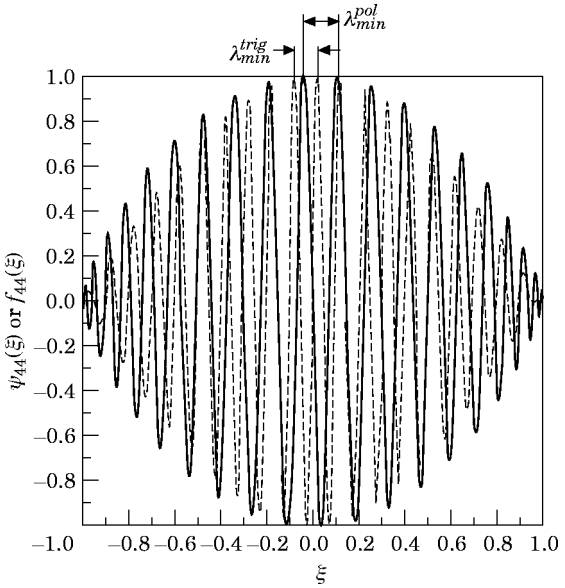

Figure 7. The minimum wavelengths λ_{min}^{trig} and λ_{min}^{pol} for the trigonometric (dashed line) and polynomial (solid line) set, respectively.

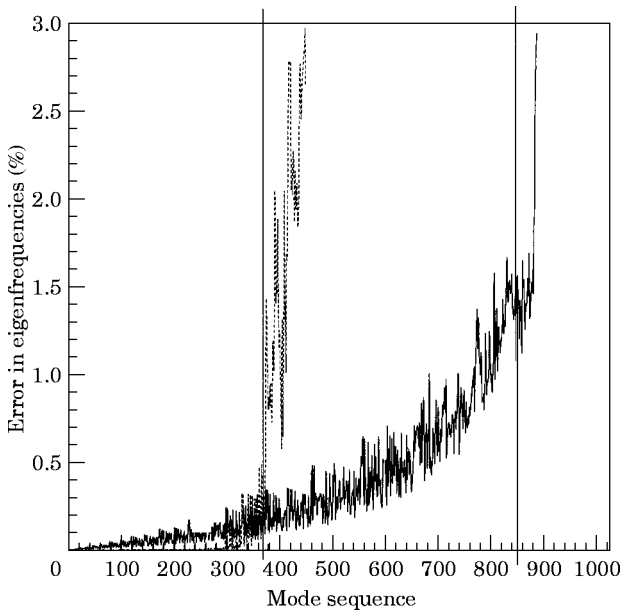

Figure 8. Errors (in per cent) on the eigenfrequencies of a S–S–S–S plate using polynomials (. . . . . .) and trigonometric (———) sets of 1024 basis functions.

successive roots. This distance is smaller near the ends and larger near the centre. Let l_{min} denote the longest distance between two successive roots of the higher order function of the functions set $\{\psi_r(\xi)\}$ or $\{f_r(\xi)\}$. It is clear that a structure mode shape having a wavelength smaller than $\lambda_{min} = 2l_{min}$ cannot be represented correctly in this basis set. Consequently, such a mode shape will have a poor convergence using this basis set. This remark leads to a *minimum wavelength* criterion that can be simply expressed for flexural waves.

For the infinite plate, the speed of flexural waves is related to the angular frequency by the classical equation.

$$c_f(\omega) = (D/\rho h)^{1/4}\omega^{1/2} \tag{25}$$

and the wavelength of flexural waves is given by

$$\lambda_f(\omega) = 2\pi c_f(\omega)/\omega = 2\pi(D/\rho h)^{1/4}\omega^{1/2}. \tag{26}$$

Using this last relation, a criterion can be used to predict the convergence rate of a given functions set. This criterion can be summarized as follows. If λ_{min} is the minimum wavelength of the functions set $\{\psi_r(\xi)\}$ or $\{f_r(\xi)\}$, only the natural flexural modes of the rectangular plate having a natural angular frequency lower than ω_{max} can be predicted, were ω_{max} is such that

$$\lambda_f(\omega_{max}) = \lambda_{min} \Rightarrow \lambda_{min} = 2\pi(D/\rho h)^{1/4}\omega_{max}^{1/2}. \tag{27}$$

Using this criterion, the convergence of the S–S–S–S plate eigenfrequencies of Figure 6 can be explained.

For the polynomials set, $\lambda_{min} = 10{\cdot}6$ cm, which leads to a $f_{max}(=\omega_{max}/2\pi) \approx 2570$ Hz corresponding to the 370th mode. For the trigonometric set, $\lambda_{min} = 7$ cm, which leads to a $f_{max} \approx 5890$ Hz corresponding to the 850th mode. This is in quite good agreement with what is shown in Figure 6.

In Figure 8, the convergence rates of the polynomials and trigonometric set are reported, in terms of percentage of error of eigenfrequencies. It can be seen that the criterion that is proposed actually allows one to predict a maximum mode order on which a convergence rate lower than 1·5% is assured.

It must be noted that for modes lower than 300, the polynomial set permits a better convergence than the trigonometric set. This is due to the fact that the trigonometric set is not a rigorously complete set. This trigonometric set presents the same behaviour as Fourier series; it is complete in the sense of the mean square convergence. However, in practice, the trigonometric set allows one to obtain a good convergence rate and to go further in the mode sequence.

4.2.3. *Convergence of mode shapes*

In Figure 9, the 370th mode shape (2571 Hz) of the S–S–S–S plate using the polynomials set is presented. It is shown that this mode shape is actually well predicted as the classical result of sine functions is retrieved with good precision, even near the edges (the convergence rate of the eigenfrequency is 0·22%).

In Figure 10, the 850th mode shape (5894 Hz) of the S–S–S–S plate using the trigonometric set is reported. It can be seen that this mode is acceptable, but there is a

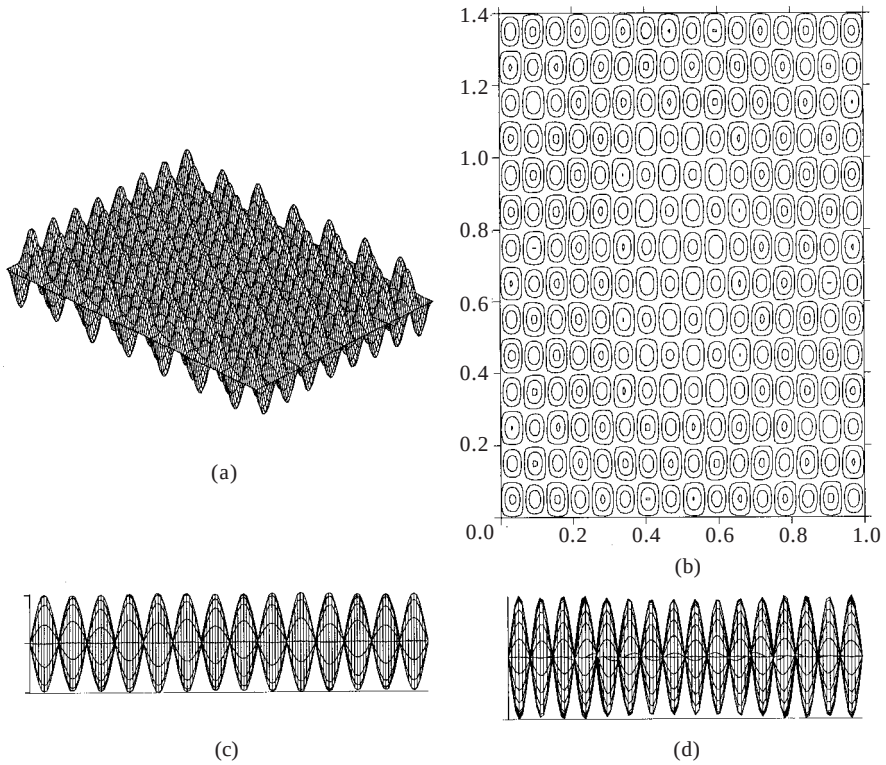

Figure 9. The mode shapes of the 370th mode of the S–S–S–S plate, using the $\{f_r(\xi)\}$ polynomial set. (a) 3-D view; (b) top view; (c) side view along y-axis; (d) side view along x-axis.

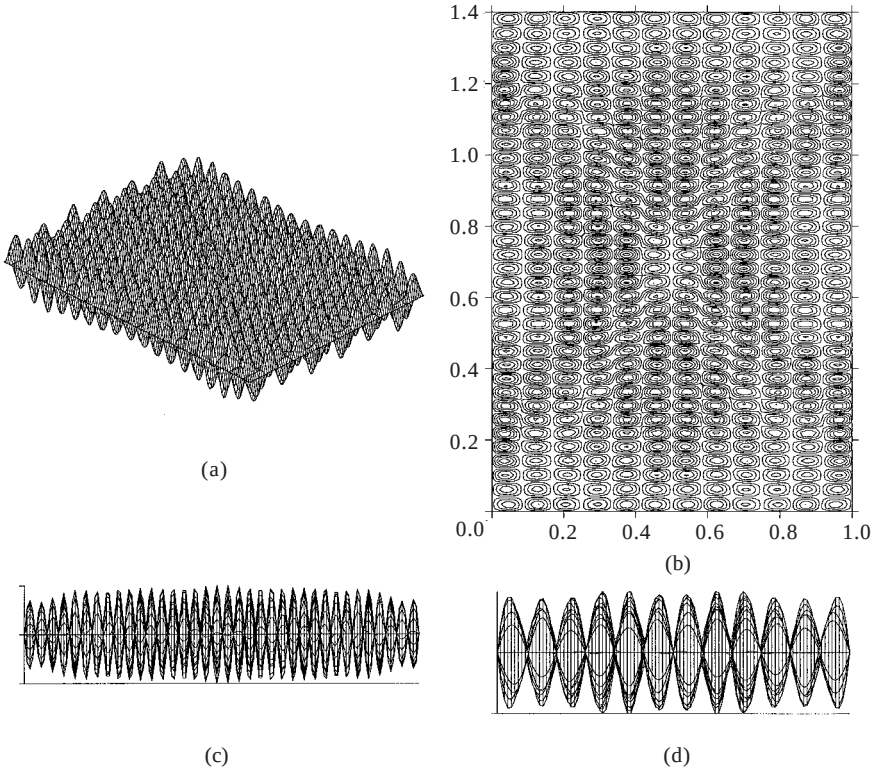

Figure 10. The mode shapes of the 850th mode of the S–S–S–S plate, using the $\{\psi_r(\xi)\}$ trigonometric set. (a)–(d) as in Figure 9.

slight lack of precision near the edges: this lack can be related to the convergence rate of the eigenfrequency which is 1·45%. However, in terms of mean quadratic velocity, such a shape will be quite acceptable. The 370th mode is reported in Figure 11 (using the trigonometric set): it can be seen that the convergence in mode shape is as good as using the polynomial set (even near the edges).

In summary, it has been shown in this section that in the case of the S–S–S–S plate, the trigonometric set allows a convergence which is at least as good as the one obtained with a polynomials set. Moreover, this trigonometric set permits us to obtain higher order modes than with polynomials, even if a small lack of precision near the edges can be observed (only for high order modes.)

4.3. THE F–F–F–F PLATE

In the same way, the natural modes of the F–F–F–F plate can be calculated by solving the eigenvalues problem (15), using the full trigonometric or polynomials set (including the first four functions in Table 3). It was done considering 1024 basis functions, selected using criterion (24).

In the case of the F–F–F–F plate, there are no analytical solutions and reference eigenfrequencies are needed to study convergence. Therefore, the reference eigenfrequencies were obtained by using the trigonometric set with 1600 basis functions.

It must be noted that using 1600 basis functions selected following the *quarter disc* criterion (24) with the plate dimensions $a = 1{\cdot}4$ m, $b = 1$ m, the maximum r order (along the x-axis) is 52 and the maximum s order (along the y-axis) is 38. Such a case is impossible to treat with polynomials using double precision since, as shown previously, polynomials are limited to order 45.

4.3.1. *Convergence of eigenfrequencies*

In Figure 12, eigenfrequencies of the F–F–F–F plate calculated using a polynomials and a trigonometric set of 1024 functions are plotted. It can be seen that trigonometric and polynomials set present the same tendencies in convergence as those observed for the S–S–S–S plate. The same *minimum wavelength* criterion can be used. However, the *minimum wavelength* is not the same as for the S–S–S–S plate. Actually, in this case, functions of order $r = 1$ and $r = 3$ have not been removed from full sets, so considering the same number (1024) of two-dimensional functions $\{\tilde{\psi}_{rs}(\xi, \eta)\}$ or $\{\tilde{f}_{rs}(\xi, \eta)\}$, the higher order for r is now 41 instead of 44. This leads to a *minimum wavelength* of 7·57 cm for the trigonometric set and 11·34 cm for the polynomials set. Then, using equation (27), the

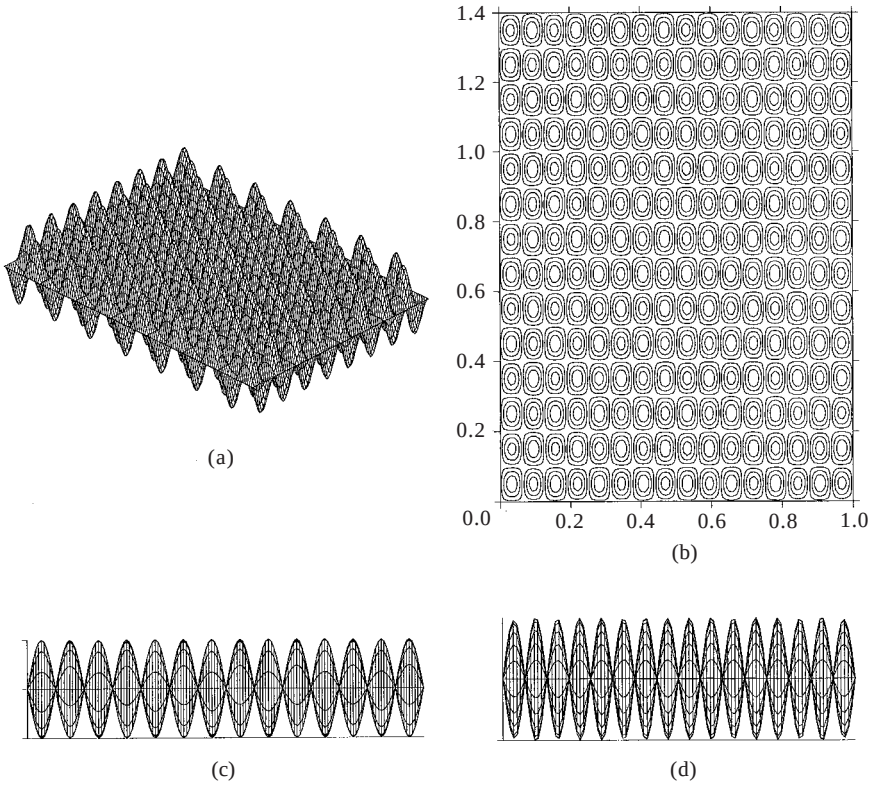

Figure 11. The mode shapes of the 370th mode of the S–S–S–S plate, using the $\{\psi_r(\xi)\}$ trigonometric set.

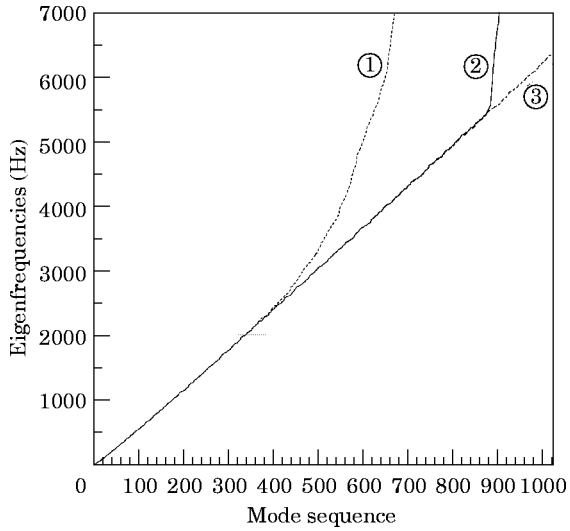

Figure 12. The convergence of eigenfrequencies of a F–F–F–F plate, using polynomials (①) and trigonometric (②) sets of 1024 basis functions. (③ is reference).

maximum accurate frequency is 5043·6 Hz ($\approx$820th mode) for the trigonometric set and 2246 Hz ($\approx$380th mode) for the polynomials set.

In Figure 13, the convergence rates (in terms of percentage of eigenfrequencies) of the polynomials and trigonometric set are compared. As it was previously mentioned, the reference eigenfrequencies are not exact values but the values obtained by using the trigonometric set with 1600 basis functions. That is why, in Figure 13, negative relative errors can be observed up to the 300th mode in the case of the polynomials set. For this

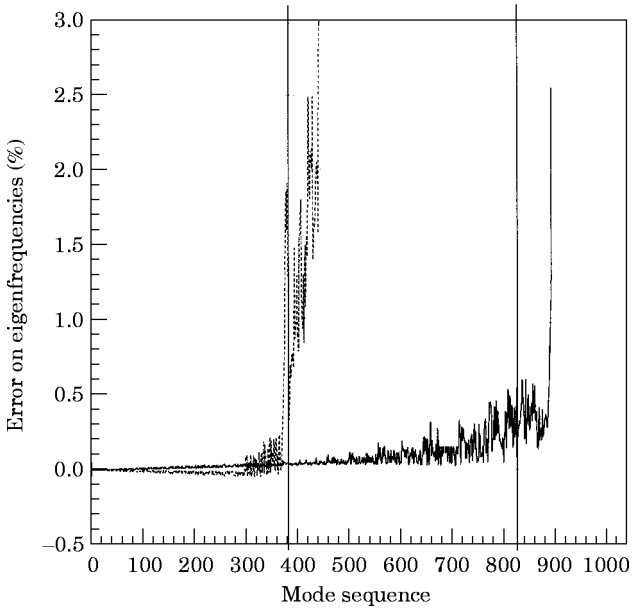

Figure 13. Errors (in per cent) on the eigenfrequencies of F–F–F–F plate using polynomials (. . . . . .) and trigonometric (———) sets of 1024 basis functions.

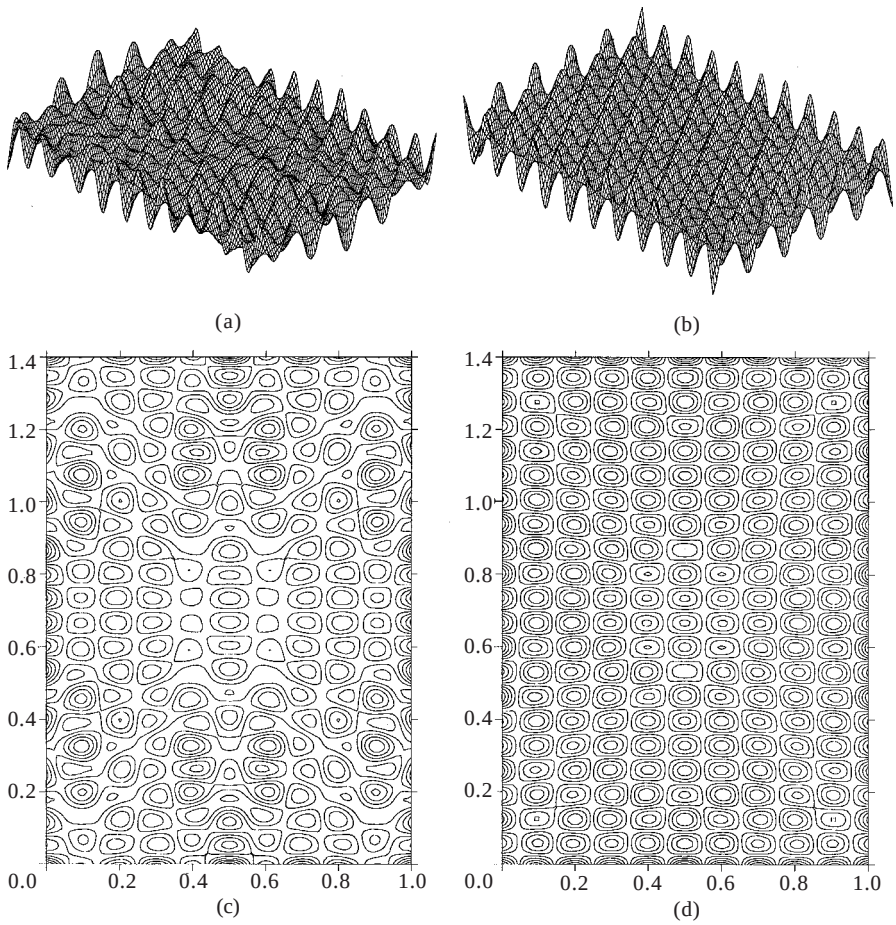

Figure 14. The shapes of the 380th eigenfunction obtained using the polynomials set ((a) and (c)) compared with the 383rd mode of the F–F–F–F plate ((b) and (d)).

first 300 modes, the polynomials set presents a better convergence than the trigonometric set even if 1600 trigonometric basis functions are used: however, over the 300th mode, the polynomials approach rapidly fails while the trigonometric approach still works up to 800th modes.

4.3.2. *Convergence of mode shapes*

In Figure 14, the mode shape of the 380th mode (at 2275 Hz) calculated with the polynomials set is presented in comparison with the reference mode shape obtained using the trigonometric set with 1600 basis functions. Using the *minimum wavelength* criterion previously exposed, this 380th mode should be converged. Looking at Figure 14, it can be seen that this is not exactly the case. Also, looking at Figure 13 it can be observed that actually, even in terms of convergence of eigenfrequency, the *minimum wavelength* criterion seems a little too optimistic in this case. However, this criterion is a good estimation since, as is shown in Figure 15, the 367th mode is actually converged. So, the *minimum wavelength* criterion has predicted the maximum order of converged modes with an error of only 3%.

In Figure 16, the 820th mode shape (at 5062 Hz) of the F–F–F–F plate calculated with the trigonometric set is compared with the reference mode shape. It can be seen that this mode converged, so for the trigonometric set, the minimum wavelength criterion is good.

In this section, it has been shown that although it is not a rigorously complete set, the $\{\psi_r(\xi)\}$ proposed trigonometric set is sufficiently complete (in the sense of the mean square convergence) to predict flexural modes of a rectangular plate. A minimum wavelength criterion permits one to predict with good accuracy the maximum mode order that can be predicted using a given functions set. Moreover, it was stated that the $\{\psi_r(\xi)\}$ set presents some additional advantages compared with polynomials.

(1) The trigonometric set can go beyond order 45, even considering the eigenvalues problem relative to plate free vibrations.

(2) For the same number of basis functions, the trigonometric set allows one to predict higher order modes than the polynomials set (≈ 800 instead of ≈ 300, considering 1024 basis functions).

(3) For a given frequency range, the trigonometric approach requires less cpu time and memory than the polynomials approach. Typically, to predict the natural modes of the

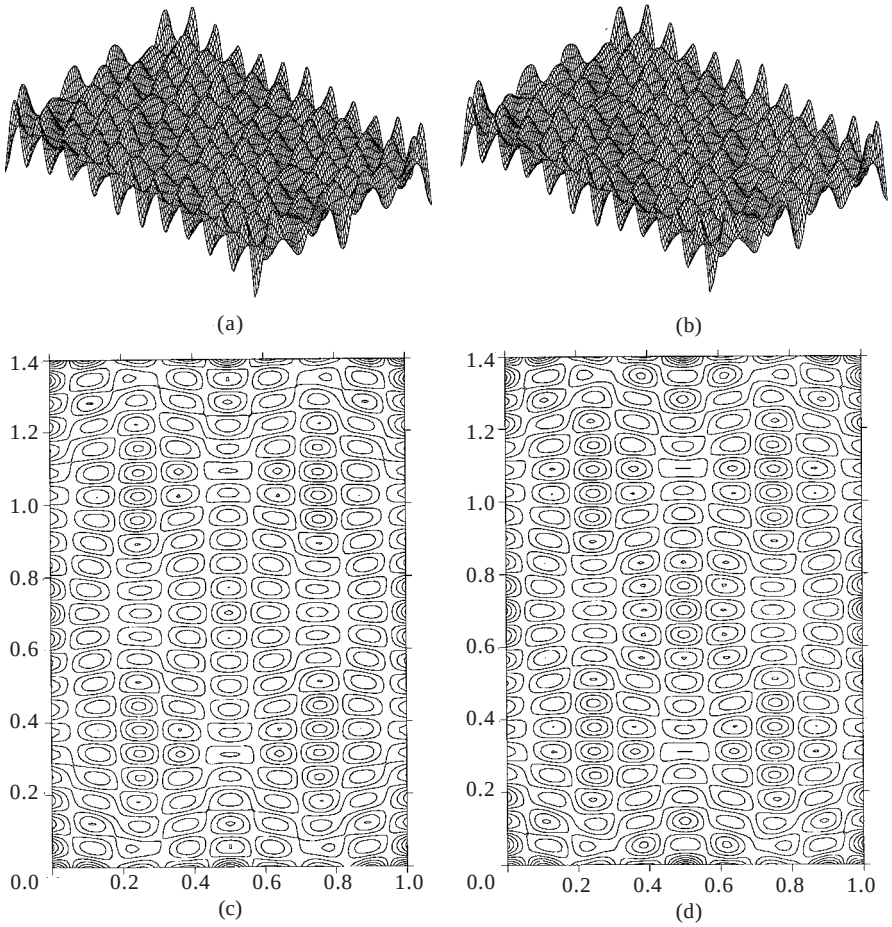

Figure 15. The shapes of the 367th eigenfunction obtained using the polynomial set ((a) and (c)) compared with the 367th mode of the F–F–F–F plate ((b) and (d)).

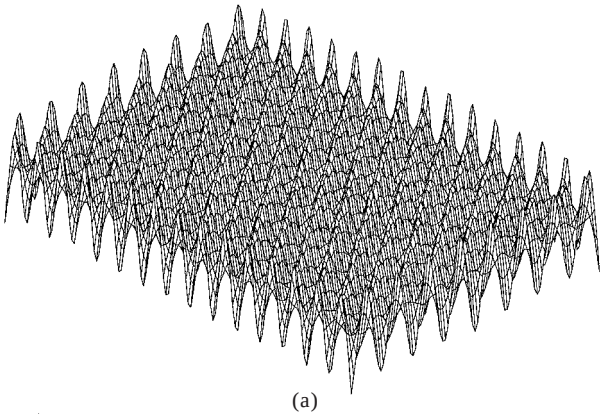

(a)

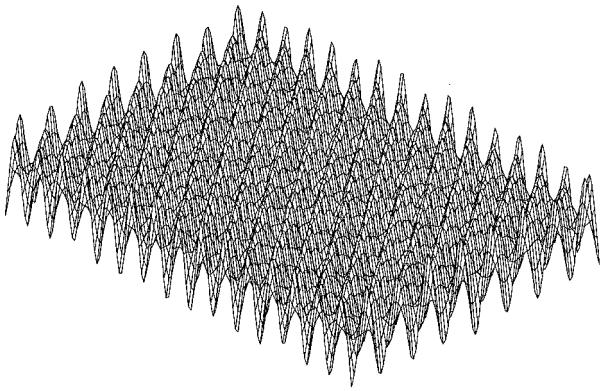

(b)

Figure 16. The 820th mode shapes of the F–F–F–F plate obtained with the trigonometric set. The comparison uses (a) 1024 and (b) 1600 basis functions.

plate presented in section 4.4.1. up to 2800 Hz, 1024 polynomials functions are required (24 MB, 13 min, 47 s*) while only 547 trigonometric functions are needed (7 MB and 1 min, 32 s*).

(4) Post-processing time can be reduced using the trigonometric set. For example, generating a mode shape file (such as the ones shown in Figure 9 and thereafter) using 1024 polynomials basis functions requires 4 min and 49 s*, while generating a mode shape file using 1024 trigonometric basis functions requires only 54 s* (a time ratio of 5·3). Moreover, using only 547 trigonometric functions permits one to obtain the same number of converged modes as when 1024 polynomials functions. Then, using 547 trigonometric functions, only 29 s* is required to generate a mode shape file (a time ratio of 9·8).

5. CONCLUSIONS

A new hierarchical functions set has been proposed in this paper which allows one to treat flexural motion of plate-like structures. This set presents all the advantages of hierarchical polynomials that can be found in the literature, particularly the fact that

* Using a 50 Megaflops, 64 MB RISC machine.

boundary conditions of an element are only defined by the first four functions. A "*minimum wavelength*" criterion was found to predict with a good accuracy the maximum mode order that can be predicted using a given functions set (trigonometric or polynomials).

Moreover, it was shown that this new basis set presents the following additional advantages that cannot be obtained from polynomials.

(1) Great numerical stability permits one to consider very high orders up to 2048 (at least) using only double precision, while polynomials fail at order 46.

(2) Convergence is better due to the fact that oscillations of trigonometric functions are regular on the entire domain $[-1, +1]$ (constant distance between two successive roots). This permits an homogeneous "*resolution*" over the entire domain, while Legendre polynomials present a high order resolution near the boundary domain and a poor resolution in the centre of the domain.

(3) Both memory and cpu time are saved since no quadruple precision pre-computed arrays are required, and only a few (and not order dependent) basic operations are needed to compute a trigonometric function.

Other basis functions could be built from trigonometric functions, dedicated to problems other than flexion waves (in plane motion, etc.). These basis functions would probably have the same properties of numerical stability and easy numerical implementation.

ACKNOWLEDGMENT

The authors wish to acknowledge C.R.S.N.G. (Canada) for support.

REFERENCES

1. A. Peano 1976 *Computers and Mathematics with Applications* **2**, 211–224. Hierarchies of conforming finite elements for plane elasticity and plate bending.
2. D. C. Zhu 1986 *Proceedings of the International Conference on Computational Mechanics*, *May* 1985, *Tokyo*. Development of hierarchal finite element methods at BIAA.
3. I. Babuska, B. A. Szabo and I. N. Katz 1981 *SIAM Journal of Numerical Analysis*. **18**, 515–545. The *p*-version of the finite element method.
4. T. Scapolla and L. Della Croce 1994 *Computer Methods in Applied Mechanics and Engineering* **111**, 185–192. Combining hierarchic high order and mixed-interpolated finite elements for Reissner–Mindlin plate problems.
5. T. Scapolla and L. Della Croce 1992 *Computer Methods in Applied Mechanics and Engineering* **101**, 43–60. On the robustness of hierarchic finite elements for Reissner–Mindlin plates.
6. J. H. Liu and K. S. Surana 1995 *Computers and Structures* **55**, 527–542. A *p*-version curved shell element based on piecewise hierarchical displacement approximation for laminated composite plates and shells.
7. M. P. Rossow and I. N. Katz 1978 *International Journal for Numerical Methods in Engineering* **12**, 977–999. Hierarchal finite elements and precomputed arrays.
8. R. H. Lyon 1975 *Statistical Energy Analysis of Dynamical Systems*: *Theory and Applications*. Cambridge, MA: MIT Press.
9. J. P. Webb and R. Abouchacra 1995 *International Journal for Numerical Methods in Engineering* **38**, 245–257. Hierarchical triangular elements using orthogonal polynomials.
10. N. S. Bardell 1991 *Journal of Sound and Vibration* **151**, 263–289. Free vibration analysis of a flat plate using the hierarchical finite element method.
11. N. S. Bardell 1989 *International Journal for Numerical Methods in Engineering* **28**, 1181–1204. The application of symbolic computing to the hierarchical finite element method.
12. N. S. Bardell 1992 *Computers and Structures* **45**(5/6), 841–874. The free vibration of skew plates using the hierarchical finite element method.
13. A. Berry, J. L. Guyader and J. Nicolas 1990 *Journal of the Acoustical Society of America* **88**,

2792–2802. A general formulation for the sound radiation from rectangular, baffled plates with arbitrary boundary conditions.
14. M. R. Spiegel 1974 *Theory and Problems of Fourier Analysis with Applications to Boundary Value Problems*. Schaum's Outline Series. New York: McGraw-Hill.
15. A. W. Leissa 1973 *Journal of Sound and Vibration* **31**, 257–293. The free vibration of rectangular plates.
16. K. M. Liew, K. Y. Lam and S. T. Show 1990 *Computers and Structures* **34**, 79–85. Free vibration analysis of rectantular plates using orthogonal plate functions.
17. S. Iguchi 1953 *Ingenieur-Archiv* **21**, Heft 5–6, 304–322. Die Eigenschwingungen und Klangfiguren der vierseitig freien rechteckigen Platte.
18. J. G. M. Kerstens 1979 *Journal of Sound and Vibration* **65**, 493–504. Vibration of a rectangular plate supported at an arbitrary number of points.
19. T. Mizusawa and T. Kajita 1987 *Journal of Sound and Vibration* **115**, 243–251. Vibration of skew plates resting on point supports.